



OPEN

Coral micro- and macro-morphological skeletal properties in response to life-long acclimatization at CO₂ vents in Papua New Guinea

Fiorella Prada^{1,12}, Leonardo Brizi², Silvia Franzellitti^{3,12}, Stefano Mengoli⁴, Simona Fermani⁵, Iryna Polishchuk⁶, Nicola Baraldi¹, Francesco Ricci⁷, Quinzia Palazzo^{5,12}, Erik Caroselli^{1,12}, Boaz Pokroy⁶, Loris Giorgini^{8,9}, Zvy Dubinsky¹⁰, Paola Fantazzini^{2✉}, Giuseppe Falini^{5,12,13✉}, Stefano Goffredo^{1,12✉} & Katharina E. Fabricius¹¹

This study investigates the effects of long-term exposure to OA on skeletal parameters of four tropical zooxanthellate corals naturally living at CO₂ seeps and adjacent control sites from two locations (Dobu and Upa Upasina) in the Papua New Guinea underwater volcanic vent system. The seeps are characterized by seawater pH values ranging from 8.0 to about 7.7. The skeletal porosity of *Galaxea fascicularis*, *Acropora millepora*, massive *Porites*, and *Pocillopora damicornis* was higher (up to ~40%, depending on the species) at the seep sites compared to the control sites. *Pocillopora damicornis* also showed a decrease of micro-density (up to ~7%). Thus, further investigations conducted on this species showed an increase of the volume fraction of the larger pores (up to ~7%), a decrease of the intraskeletal organic matrix content (up to ~15%), and an increase of the intraskeletal water content (up to ~59%) at the seep sites. The organic matrix related strain and crystallite size did not vary between seep and control sites. This multi-species study showed a common phenotypic response among different zooxanthellate corals subjected to the same environmental pressures, leading to the development of a more porous skeletal phenotype under OA.

Tropical coral reefs support the livelihoods of hundreds of millions of people around the world, harbor 25% of all marine species, and protect thousands of kilometers of shoreline from waves and storms¹. However, coral reefs face an intensifying array of threats deriving from pollution and overexploitation which is leading to a decline in their health². In addition, global climate change compounds these threats in multiple ways. Increases in seawater CO₂ and associated decreases in carbonate ion concentration, known as ocean acidification (OA), are projected

¹Marine Science Group, Department of Biological, Geological and Environmental Sciences, University of Bologna, Via F. Selmi 3, 40126 Bologna, Italy. ²Department of Physics and Astronomy, University of Bologna, Viale Berti Pichat 6/2, 40127 Bologna, Italy. ³Animal and Environmental Physiology Laboratory, Department of Biological, Geological and Environmental Sciences, University of Bologna, via S. Alberto 163, 48123 Ravenna, Italy. ⁴Department of Management, University of Bologna, Via Capo di Lucca 34, 40126 Bologna, Italy. ⁵Department of Chemistry 'Giacomo Ciamician', University of Bologna, Via F. Selmi 2, 40126 Bologna, Italy. ⁶Department of Material Sciences and Engineering and the Russell Berrie Nanotechnology Institute, Technion – Israel Institute of Technology, Haifa, Israel. ⁷School of BioSciences, University of Melbourne, Parkville 3010, Australia. ⁸Department of Industrial Chemistry "Toso Montanari", University of Bologna, Viale Risorgimento 4, 40136 Bologna, Italy. ⁹Interdepartmental Center for Industrial Research on Advanced Applications in Mechanical Engineering and Materials Technology, CIRI-MAM, University of Bologna, Viale Risorgimento 2, 40136 Bologna, Italy. ¹⁰The Mina and Everard Goodman Faculty of Life Sciences, Bar-Ilan University, 52900 Ramat-Gan, Israel. ¹¹Australian Institute of Marine Science, PMB 3, Townsville, QLD 4810, Australia. ¹²Fano Marine Center, The Inter-Institute Center for Research on Marine Biodiversity, Resources and Biotechnologies, Viale Adriatico 1/N, 61032 Fano, Italy. ¹³Consiglio Nazionale delle Ricerche, Istituto per lo Studio dei Materiali Nanostrutturati (CNR-ISMN), Via P. Gobetti 101, 40129 Bologna, Italy. ✉email: paola.fantazzini@unibo.it; giuseppe.falini@unibo.it; s.goffredo@unibo.it

to have profound implications for marine calcifiers, as carbonate ions are essential for biotic calcification³. Coral responses to OA may be affected by several factors including colony morphology, size, skeletal mineralogy and structure, tissue thickness, symbiont types, and/or the mechanisms of nutrient acquisition⁴. Moreover, the discrepancy among responses could derive from different experimental designs and analytical methods (e.g., addition of acid vs CO₂ bubbling to mimic OA), co-limiting environmental conditions (e.g., temperature, light intensity, flow, feeding, etc.), and exposure times (days to months or even life times)⁵.

To date, most studies both under controlled conditions and under natural conditions in the field (e.g., CO₂ vents), support predictions of decreased rates of calcification and increased rates of dissolution and bioerosion as seawater pH decreases⁶. However, studies conducted using skeletal cores have shown that coral calcification rates have not declined at a constant rate as ocean pH decreased and temperatures warmed throughout the twentieth century. On the contrary, at some locations, calcification rates have remained stable and in others they have even increased over this time period^{7–9}. Even where declines in calcification have occurred, many other factors such as ocean warming, sea level rise, changes in surface ocean productivity, as well as many localized anthropogenic disturbances co-occur with OA. These additional factors also influence coral growth and could obscure our ability to attribute changes in coral calcification solely to OA¹⁰.

Most of the available knowledge about OA effects on marine organisms derives from short-term laboratory or mesocosm experiments on isolated organisms¹¹, which can substantially underestimate full organism acclimatization¹². In fact, taxa that appear unaffected by high CO₂ under controlled conditions may be: (1) vulnerable in the long-term¹³, (2) affected during life stages that were not considered during the experiment¹⁴, or (3) be indirectly affected by OA-driven ecological changes (e.g., food webs, competition, diseases and/or community structures, habitat properties such as microbial surface biofilms)¹⁵. Likewise, other taxa that respond negatively to OA under controlled conditions may be capable of acclimatizing in the longer term. Thus, field experiments, where organisms are naturally exposed to OA for their entire life, as found around submarine CO₂ vents, could provide important new insights. However, vent systems are not perfect predictors of future ocean ecology owing to temporal variability in pH, spatial proximity of populations unaffected by acidification, and the unknown effects of other changing parameters (e.g., temperature, currents)¹⁶. Nonetheless, vents acidify sea water on sufficiently large spatial and temporal scales to integrate ecosystem processes such as reproduction, competition and predation¹⁷. Field-based studies conducted at volcanic CO₂ seeps in Italy^{17–19}, Japan²⁰, Mexico²¹, and Papua New Guinea (PNG)¹⁵ provide a unique opportunity to investigate long-term effects of OA on marine ecosystems that have been naturally exposed to chronic low pH and concomitant altered carbonate chemistry parameters for years/decades. These studies have already demonstrated substantial changes in community structure and functional biodiversity²² of benthic species, as well as an array of responses to OA spanning from sharp decrease to no effect on calcification rate²³.

Studies conducted on corals at volcanic CO₂ vents in Papua New Guinea (PNG) have supported the mixed effects observed in laboratory experiments^{15,24}. Hard coral cover is similar at acidified and control sites (33% versus 31%). However, the cover of massive *Porites* is doubled under OA, whereas the cover of more structurally complex corals is reduced by one third²⁴. Some species are significantly less common or even absent under OA. For instance, while the coverage of *Pocillopora damicornis* decreases by 43% in acidified sites, in situ growth measurements have found small differences in linear extension rate¹⁵, but large differences in recruitment success²⁵. Population reductions in situ, combined with observations of negative physiological impacts, including declines in calcification under OA, strongly suggest that low pH imposes selection pressure on less resilient taxa within the PNG system²³.

The aim of this study was to assess the effects of long-term exposure to OA on the skeletal parameters (micro-density, porosity, bulk density) of four tropical zooxanthellate coral species *Galaxea fascicularis* (Linnaeus, 1767), *Acropora millepora* (Ehrenberg, 1834), massive *Porites* Link, 1807, and *P. damicornis* (Linnaeus, 1758), living at CO₂ vents and adjacent control sites in Milne Bay Province, PNG¹⁵. Additional macroscale and microscale skeletal analyses, namely Time-Domain Nuclear Magnetic Resonance (TD-NMR), Thermogravimetric Analysis (TGA), and synchrotron high-resolution powder X-ray diffraction (HRPXRD) analyses were performed on *P. damicornis*, the only species displaying differences in micro-density at the seep sites compared to control.

Materials and methods

Study sites and coral sampling. The study was conducted at two shallow-water (1–5 m) volcanic CO₂ seeps at ambient temperature and adjacent control sites at Milne Bay Province, PNG, namely Dobu and Upa Upasina (Fig. 1). Almost pure CO₂ (~99%) has been streaming from the seabed for an unknown period of time (confirmed for approximately 70 years, but likely much longer)¹⁵, resulting in localized acidified conditions. Environmental parameters (measured: pH, dissolved inorganic carbon, total alkalinity, salinity, and temperature; calculated with CO2SYS software: pCO₂ and aragonite saturation state) were obtained across a 4-year period (2010–2013) at 1–5 m depth in both control and seep sites^{15,24}. Two-cm coral fragments, which corresponds to approximately a 1.5-year growth increment in all the investigated species^{15,26,27}, were collected at 1–5 m depth from adult colonies of *P. damicornis*, *G. fascicularis*, *A. millepora*, and massive *Porites* at control and seep sites in August 2010 (N = 6–15 fragments per site, each fragment from a different colony)²⁸. Tissue from the coral fragments was totally removed using established protocols applied in previous studies on corals which include immersing the samples in a solution of 10% commercial bleach for 3 days and drying them for 24 h at a maximum temperature of 40°C^{29–32}. Dried fragments were kept in codified Eppendorf tubes prior to skeletal measurements.

Skeletal porosity, bulk density, and micro-density determination. The skeletal porosity, bulk density, and micro-density of the 192 fragments from the control and seep sites at Dobu and at Upa Upasina were



Figure 1. Maps of Papua New Guinea and the two study locations (Dobu and Upa Upasina) on Normanby and Dobu Islands, Milne Bay Province. This Figure was created using Adobe Photoshop CC 2018 (<https://www.adobe.com/products/photoshop.html>) with imagery from Google Earth (V 9.140.0.4. Eye alt 45 km. SIO, NOAA, U.S. Navy, NGA, GEBCO. TerraMetrix 2020, Digital Globe 2020. <https://earth.google.com>. 10 December 2020). The inset map was made modifying an image freely available at the following website: https://d-maps.com/carte.php?num_car=3336&lang=en.

obtained as follows. After determining the dry mass, the fragments were placed inside a drying chamber connected to a vacuum pump to evacuate air and water from the pores, a necessary step in order to allow effective saturation of the samples in the following phase. After 3 h, distilled water was gently introduced to fully saturate the samples which were then weighed in air to determine the saturated weight. Buoyant weight was then measured with a hydrostatic balance (Ohaus Explorer Pro balance ± 0.0001 g) equipped with a density determination kit and used to calculate porosity, bulk density, and micro-density by means of standard calculations (details in Supplementary Methods)²⁹.

Time-domain nuclear magnetic resonance for pore size distribution determination. To investigate the distribution of pore-size classes, through the analysis of the NMR transverse relaxation time T_2 distributions from control and seep site (details in Supplementary Methods), coral fragments still fully saturated with water, were placed on a wet paper to dry the excess of water on their surface. Then, every fragment was put inside a glass tube, sealed and immediately inserted into the magnetic field to be subjected to TD-NMR measurement. A home-built relaxometer based on an electromagnet JEOL C-60 (magnetic field $B_0 = 0.5$ Tesla) with a radiofrequency coil ≈ 8 mm in diameter, and equipped with a Spinmaster portable console (Stelar, Mede, Pavia, Italy) was used. The Carr-Purcell-Meiboom-Gill (CPMG) sequence with 200 μ s echo time was used to acquire for each specimen the transverse relaxation curve. The measured multi-exponential relaxation curves, affected by unavoidable measurement noise, were transformed into distributions of the transverse relaxation time T_2 by the algorithm UPEN (Uniform-Penalty inversion algorithm)³³, implemented in the UpenWin software³⁴. The ratio between the signal under a particular portion of the T_2 distribution and the total acquired signal will correspond to the ratio of the volume of the pores with a particular pore size to the total pore volume. TD-NMR measurements were performed on 2 fragments per site per species for *A. millepora*, massive *Porites*, and *G. fascicularis* and on all available fragments of *P. damicornis* (a total of 60 fragments). The T_2 distributions showed a cut-off at 3 ms allowing to divide the pores containing water into two classes, distinguishing the smaller pores (smaller volumes, estimated pore sizes < 1 μ m) from the remaining larger ones (larger volumes, estimated pore sizes > 1 μ m). For the sake of simplicity, the two classes were named micro-scale and macro-scale pores^{13,35}.

Thermogravimetric analysis for organic matrix content determination. To determine the intraskeletal organic matrix and water content, thermal gravimetric measurements were performed using a TA Instruments thermobalance model SDT-Q600 with 0.1 μ g of balance sensitivity. Powdered subsamples (5 to 10 mg), held in alumina pans, were heated under a linear gradient from ambient (ca. 20 °C) up to 600 °C with an isotherm at 120 °C for 5 min to remove the adsorbed water; heating rate: 10 °C/min under an N_2 atmosphere,

with flux fixed to 100 ml/min. Two main weight loss regimes were identified: a first one in a range around 125–250 °C (related to the loss of structured water molecules) followed by another thermal region between 250 and 470 °C (generally associated with organic matrix pyrolysis)³⁶. A total of 32 fragments from the control and seep sites at Dobu (10 for each site) and at Upa Upasina (6 for each site) were analyzed.

Synchrotron high-resolution X-ray powder diffraction. To determine crystallite parameters, coral fragments were measured at the ID22 beamline of the European Synchrotron Radiation Facility (Grenoble, France) using a wavelength of 0.4 Å (details in Supplementary Methods). Subsamples of the fine powder were loaded into borosilicate glass capillaries of 0.7–1 mm in diameter and measured at room temperature, and again after ex-situ heating at 300 °C for 2 h, to remove the organic matrix effects on the strain³⁷. Rietveld refinement was used to calculate the unit-cell parameters from the diffraction pattern profiles. The line profile analysis was applied to a specific diffraction peak to obtain the coherence length (nm) along various crystallographic directions, which was achieved by fitting the profile to a Voigt function and deconvoluting the Lorentzian and Gaussian widths. Analyses were conducted on fragments of *P. damicornis* from Upa Upasina in the control (N = 3) and seep (N = 3) site.

Statistical analyses. Permutation multivariate analysis of variance (PERMANOVA) was performed using PRIMER v6³⁸ and based on Euclidean distances (999 permutation) to test for (1) variations of environmental parameters amongst locations and sites; (2) variations of skeletal parameters amongst locations, sites, and species. When the main tests revealed statistical differences ($P < 0.05$), PERMANOVA pairwise comparisons were carried out. The BEST routine in PRIMER v6 (999 permutations) was carried out to check for auto-correlated environmental variables, thus obtaining the minimum subset of variables that may explain differences in environmental conditions amongst locations, sites and seasons (i.e., Spring included data collected in April and May; Winter included data collected in January and December). Organic matrix related strain and crystallite size in *P. damicornis* were compared between control and seep sites using the non-parametric Mann–Whitney U-test, due to deviations from parametric t-test assumption (Normality: Shapiro–Wilk’s test; equal variance: Levene’s test). This statistical analysis was performed using SPSS 20.0. Data visualization and graphics were obtained with the ggplot2 package in R³⁹. Statistical differences were accepted when $P < 0.05$.

Results

Environmental parameters. The values of the environmental parameters collected at control and seep sites in Dobu and Upa Upasina over a 3-year period are summarized in Fig. S1. Briefly, pH and pCO₂ across both seep sites averaged 7.72 ± 0.23 (SD) and 1133 ± 1161 μatm , while at the control sites it averaged 7.93 ± 0.10 and 518 ± 250 μatm , respectively. The complete dataset of environmental parameters (Fig. S1) was analyzed to test for differences between sampling locations, and between control vs seep sites within each location. Effects of seasonality were also considered. PERMANOVA analyses showed that environmental conditions were different between locations and sites and that seasons did not differ significantly (Supplementary Table S1 and Fig. S1). PERMANOVA pair-wise comparisons showed that within each of the two locations control and seep sites were significantly different (Dobu: $t = 3.127$, $P = 0.001$; Upa Upasina: $t = 2.547$, $P = 0.001$). The two control sites also differed between the two locations ($t = 2.112$, $P = 0.002$), while seep sites were similar ($t = 1.244$, $P = 0.154$). The BEST routine revealed that pCO₂ and Ω_{AR} were strongly autocorrelated with the other environmental parameters ($\text{Rho} = 0.995$, $P = 0.001$) and were therefore excluded from the following PERMANOVA analysis. PERMANOVA analyses on single environmental parameters showed that pH and total alkalinity were significantly different between control and seep sites, while temperature was significantly different between locations (Table 1 and Supplementary Table S1). DIC was significantly different between controls of Upa Upasina and Dobu ($t = 6.137$, $P = 0.001$) while at the seep sites DIC was homogeneous ($t = 0.061$, $P = 0.962$). Salinity was unchanged between either locations or sites (Table 1 and Supplementary Table S1).

Skeletal parameters in corals sampled at the control and seep sites of Dobu and Upa Upasina. Results for bulk density, micro-density, and porosity are reported in Fig. 2 and in Supplementary Table S2. PERMANOVA analyses indicated significant differences among species in micro-density, porosity, and bulk density (Table 2). Porosity and bulk density were also significantly different between sites (Table 2). For all species, porosity and bulk density were significantly different between control and seep sites at Upa Upasina ($t = 4.752$, $P = 0.001$ and $t = 5.864$, $P = 0.001$, respectively), with higher porosity and lower bulk density at the seep site compared to the control (Fig. 2). Bulk density was significantly lower at the seep site compared to the control also at Dobu ($t = 2.675$, $P = 0.010$; Fig. 2). Micro-density showed a significant interaction between the factor Site and Species (Table 2); indeed micro-density values assessed in *P. damicornis* were significantly lower at the seep site compared to the control at both locations (Fig. 2; Table 3).

Micro-density changes in *P. damicornis* were further explored both statistically and through additional macroscale and microscale skeletal analyses. Specifically, Time-Domain Nuclear Magnetic Resonance (TD-NMR), Thermogravimetric Analysis (TGA), and synchrotron high-resolution powder X-ray diffraction (HRPXRD) analyses were performed. TD-NMR measurements were performed on two fragments for all species to have a general overview of the T_2 distributions (Supplementary Fig. S2). Further analyses were conducted on all available fragments of *P. damicornis* to quantify macro-scale pore volume fraction. PERMANOVA analyses showed that macro-scale pore volume fraction was significantly higher at the seep site compared to the control in both locations (Upa Upasina: $t = 2.126$, $P = 0.041$; Dobu: $t = 2.549$, $P = 0.028$; Fig. 3 and Supplementary Table S3). The intraskeletal organic matrix (OM; $t = 4.856$, $P = 0.004$) and water content ($t = 4.891$, $P = 0.001$) were significantly different between Sites only at Upa Upasina (Table 4; Fig. 3; Supplementary Table S4). In particular, the former

Location	Dobu		Upa Upasina	
Site	Control	Seep	Control	Seep
pH	7.96 (0.04)	7.66 (0.27)	7.91 (0.13)	7.75 (0.19)
	N = 46	N = 130	N = 67	N = 222
	a	b	a	b
DIC	1946 (15)	2106 (90.0)	2082 (38)	2060 (30.0)
	N = 32	N = 30	N = 71	N = 254
	a	b	c	b
TA	2235 (9)	2275 (1)	2252 (21)	2285 (18)
	N = 47	N = 207	N = 71	N = 254
	a	b	a	b
Salinity	34.9 (0.8)	34.7 (0.7)	35.2 (0.8)	34.8 (0.7)
	N = 59	N = 207	N = 71	N = 254
	a	a	a	a
T (°C)	29.1 (1.4)	29.0 (0.7)	30.1 (1.3)	30.2 (0.9)
	N = 59	N = 207	N = 71	N = 242
	a	a	b	b

Table 1. Means and standard deviation (in parenthesis) of the investigated environmental parameters in seep and control sites in Dobu and Upa Upasina. Lettering indicates significantly different groups (PERMANOVA on single parameters). pH_{TS} pH in total scale, pCO_2 carbon dioxide partial pressure, Ω_{AR} aragonite saturation, DIC dissolved inorganic carbon, TA total alkalinity, T seawater temperature, N number of measurements.

showed lower values at the seep site compared to control, while the latter showed the opposite trend (Fig. 3). The intraskeletal OM content was significantly different also among locations (Table 4).

Three *P. damicornis* skeletal fragments from the control and from the seep sites in Upa Upasina were analysed by HRPXRD. All HRPXRD patterns were well indexed as aragonite and no additional diffraction peaks were detected. Then, the peaks were refined using the Rietveld method⁴⁰ and lattice parameters and strain (Supplementary Table S5), and microstructural data⁴¹, crystallite size, and microstrain (Supplementary Table S6), were calculated. No significant differences were found between the control and seep site. To test the influence of the OM on the mineral strain, ex-situ heat treatments prior the HRPXRD measurements, which remove the effect of the OM on the strain³⁷, were performed. The data showed that OM induced a positive strain on *a*- and *c*-axis and a negative one on the *b*-axis, but no significant differences were found between the control and seep site (Supplementary Table S5). We also measured crystallite size after the thermal annealing together with the transition to calcite (Supplementary Tables S5 and S6). These latter parameters did not show any significant difference between the control and seep sites.

Discussion

In the past decades, significant efforts have been made to quantify the ecological effects of ongoing ocean acidification (OA) in tropical regions. However, assessing the effects of OA on reef-building corals poses major challenges because multiple environmental changes, including ocean warming, are co-occurring with OA, impacting coral growth^{42,43}. This study investigated the effects of long-term exposure to elevated CO_2 on skeletal properties in tropical zooxanthellate corals naturally living at CO_2 vents.

Similar to Mediterranean¹³ and other tropical coral species⁴⁴, increased porosity and decreased bulk density was observed at the seep sites compared to the control sites, with some species showing more marked trends than others, in agreement with a general decreasing trend of net calcification rates at relatively low pH conditions resembling IPCC projections^{15,45}. A 2-year field transplant experiment conducted on *Porites astreoides*, *Siderastrea siderea* and *Porites porites* at low pH submarine springs in the Yucatán peninsula (Mexico) showed species-specific OA-related vulnerability in calcification rates which may be linked to differential growth rates, with fast-growing corals being likely more sensitive to low carbonate ion availability⁴⁶. Species-specific sensitivities to OA also depend on its impacts on chemistry within the calcifying fluid^{47,48} and/or in the diverse use of metabolic reserves⁴⁹. Moreover, different populations of the same species might display variable responses to OA, as highlighted for instance by the intra-specific variability displayed by calcification rates of *Acropora digitifera* from two distinct locations after exposure to acidified conditions in aquaria⁵⁰. All these aspects could contribute to explain the variability observed by the different species in the two locations considered in the current study.

Micro-density showed lower values at the seep sites compared to the control sites of both locations only in *P. damicornis*. Micro-density, which represents the mass per unit volume of the biogenic calcium carbonate composing the skeleton⁵¹, depends on the mineral composition of the skeleton and on intraskeletal organic matrix (OM) and water content²⁹. The evaluation of additional macro- and micro- scale parameters performed in this species also revealed an increase in macro-scale pore volume fraction and intraskeletal water content and a decrease in OM, and eventually strong linked water³⁶. In particular, the observed increase of intraskeletal water content at the seep site can partially justify the observed decrease in skeletal micro-density. According to literature, the observed decrease of skeletal micro-density could also stem from a variation in chemistry and micro-architecture

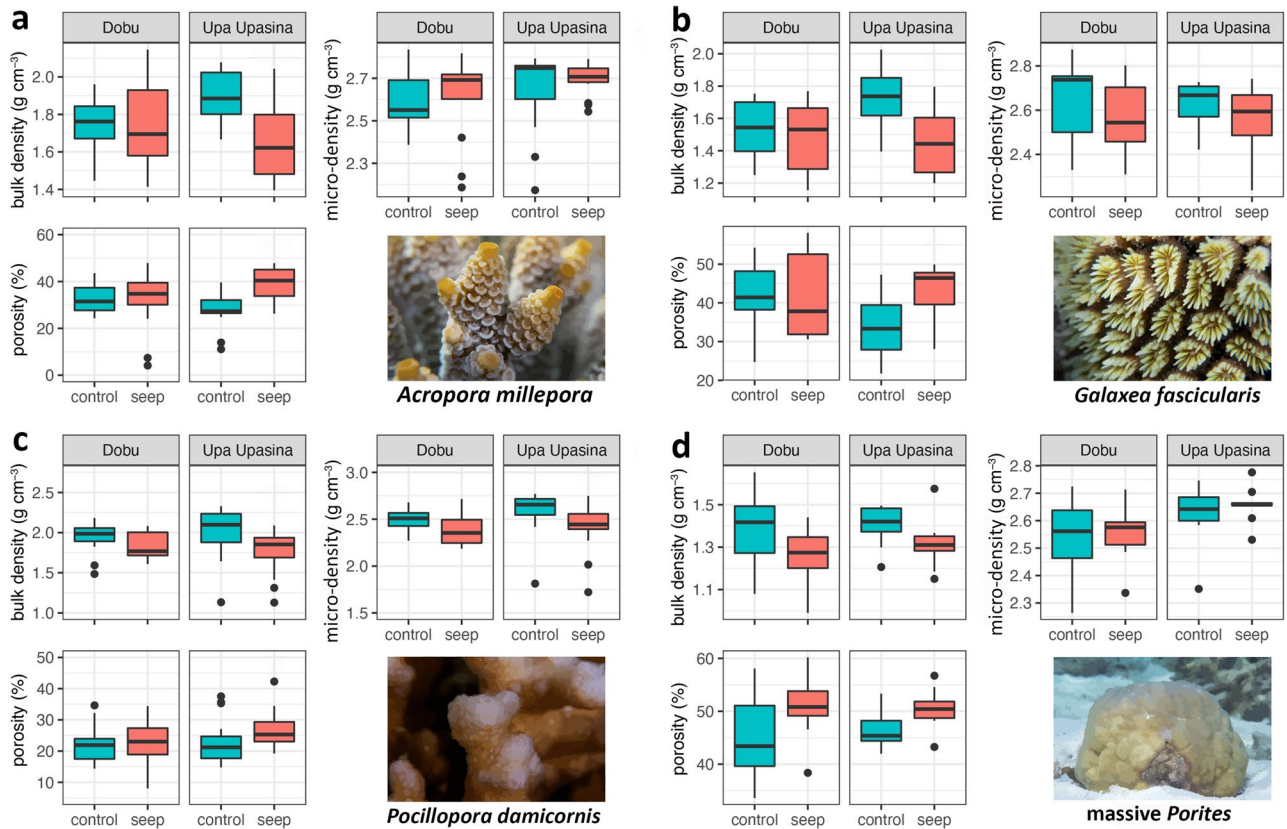


Figure 2. Skeletal parameters micro-density, porosity and bulk density at control (green box plots) and seep sites (pink box plots) in Dobu and Upa Upasina (UPA) for (a) *Acropora millepora*, (b) *Galaxea fascicularis*, (c) *Pocillopora damicornis*, and (d) massive *Porites*. The boxes indicate the 25th and 75th percentiles and the line within the boxes mark the medians. Whisker length is equal to $1.5 \times$ interquartile range (IQR). Circles represent outliers. Statistical analyses for these data are reported in Tables 2 and 3. Plots were created with the R package ggplot2⁶². Photographs by co-author FR.

	df	Porosity		Bulk density		Micro-density	
		Pseudo-F	P	Pseudo-F	P	Pseudo-F	P
Sp	3	61.541	0.001	78.244	0.001	10.096	0.001
Lo	1	0.034	0.853	3.791	0.054	8.732	0.007
Si(Lo)	2	10.374	0.001	20.775	0.001	2.645	0.073
SpxLo	3	0.276	0.841	0.174	0.922	1.487	0.223
SpxSi(Lo)	6	0.850	0.546	1.211	0.327	3.535	0.006

Table 2. Results of the PERMANOVA analysis for porosity, bulk density, and micro-density in the control and seep sites at Dobu and Upa Upasina for *Acropora millepora*, *Galaxea fascicularis*, *Pocillopora damicornis*, and massive *Porites*. Significant values are reported in bold. Sp species, Lo location, Si site.

	Upa Upasina		Dobu	
	t	P	t	P
<i>Acropora millepora</i>	1.002	0.375	0.815	0.440
<i>Galaxea fascicularis</i>	1.092	0.291	0.802	0.424
massive <i>Porites</i>	0.813	0.488	0.476	0.650
<i>Pocillopora damicornis</i>	4.787	0.002	3.615	0.003

Table 3. PERMANOVA pairwise comparisons for micro-density based between Control and Seep sites within locations (Dobu and Upa Upasina) for the four investigated species. The pairwise test was conducted only for micro-density based on the significant interaction between Site and Species (Table 2). Significant values are reported in bold.

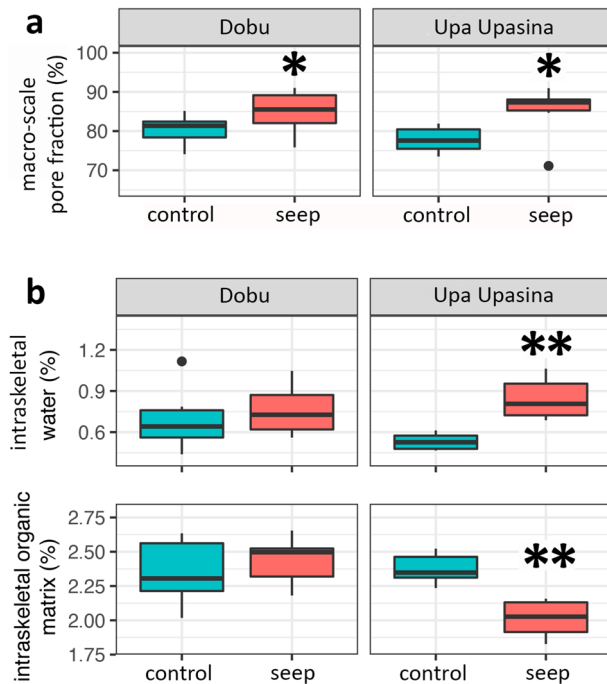


Figure 3. Macro-scale pore volume fraction (in the figure simply macro pore fraction) and intraskeletal OM and water content for *P. damicornis* from control and seep sites at Dobu and Upa Upasina. **(a)** Time Domain-Nuclear Magnetic Resonance measurement of macro-scale pore volume fraction. **(b)** Thermogravimetric Analysis of microscale parameters, namely intraskeletal organic matrix (OM), intraskeletal water content, and total (the sum of OM and water). The box indicates the 25th and 75th percentiles and the line within the box marks the median. Whisker length is equal to $1.5 \times$ interquartile range (IQR). Circles represent outliers. Significant differences between control and seep sites are represented by asterisks, ** $P < 0.01$, * $P < 0.05$. Plots were created with the R package ggplot2⁶².

Factor	df	Pseudo-F	P
Intraskeletal water content			
Lo	1	0.279	0.608
Si(Lo)	2	6.831	0.005
Intraskeletal organic matrix content			
Lo	1	12.318	0.001
Si(Lo)	2	7.164	0.002
Macro-scale pore volume fraction			
Lo	1	0.775	0.380
Si(Lo)	2	5.715	0.012

Table 4. Results of the PERMANOVA analysis for intraskeletal water and organic matrix (OM) content and macro-scale pore fraction volume in *Pocillopora damicornis* in control and seep sites at Dobu and Upa Upasina. Lo location, Si site.

of the skeleton⁵², the presence of occluded nano-porosity¹³, and the presence of amorphous calcium carbonate⁵³. Changes in OM and water content with pH reduction have been previously reported, showing either an increase in the tropical *Stylophora pistillata* kept in aquaria at pH 7.2 for approximately 1 year^{36,44}, or no variation in the temperate *Balanophyllia europaea* naturally living along a CO₂ vent at average seawater pH 7.7³². Moreover, *P. damicornis* exposed to pH 7.8, 7.4 and 7.2 in aquaria for 3 weeks showed a 4 to 70-fold up-regulation of genes encoding skeleton organic matrix proteins at all pH treatments⁵⁴. In these studies, the observed up-regulation of genes linked to OM proteins and the increase in OM content was hypothesized to promote calcification under less favorable acidified conditions. Thus, the observed decline in OM in *P. damicornis* in the current study suggests a possible decline in net calcification rates at the seep site, which is in agreement with the observed increase in skeletal porosity. However, considering the natural setting in which the study was performed, we cannot exclude

the influence of other covarying environmental factors in determining the observed responses (e.g., turbidity, light availability, organic/inorganic nutrient availability, feeding)^{55–58}.

The decrease of intra-skeletal OM content in samples from seep sites was not associated with a significant change in strain, micro-strain, or crystallite size. These observations may indicate that the amount of intra-crystallite OM does not change since the crystallite sizes after the thermal annealing are the same for samples from the control and the seep sites. Thus, the observed decrease in OM is likely associated with a decrease in the inter-crystallite OM. In addition, the stability of aragonite through the transition to calcite and the lattice parameters of the calcite formed after thermal annealing did not show a significant difference between control and seep samples. The crystallographic features of aragonite from coral skeletons have been previously investigated⁵⁹. The reef building coral *Stylophora pistillata* grown in aquaria under different experimental seawater acidification (pH 8.2, 7.6, and 7.3) showed anisotropic distortions of aragonite lattice parameters and a reduction of the crystallite sizes under acidified conditions³⁶. In the presented study, these parameters were unaffected by decreasing pH, suggesting that biological control over calcification does not change at the nanoscale, as reported for *B. europaea*¹³. The fact that different species were used, but most of all that *S. pistillata* was exposed for 1 year (short-term acclimation) while in the current study species were exposed to acidified conditions for generations (life-long acclimatization) likely accounts for these discrepancies. The calcite phase obtained by annealing of coral samples has similar lattice parameters in samples from the control and seep sites. These parameters, when compared with those of synthetic calcite⁶⁰, did not show differences. A different behavior was observed for calcite obtained from *Desmophyllum* and *Favia* aragonitic skeletons, which showed different strain compared with geological or synthetic calcite⁵⁹.

Conclusions

This multi-species study showed a common phenotypic response among four zooxanthellate corals which displayed a more porous skeletal phenotype under OA. Additionally, these skeletal macromorphological adjustments led to decreased micro-density in *P. damicornis* but did not affect the measured crystallite features, suggesting that the fundamental structural components produced by the biomineralization process might be substantially unaffected by increased acidification^{13,61}. Nonetheless, the porous phenotype here described may render structurally complex and massive corals more vulnerable to damage and bio-erosion under climate change, which in the future may lead to a weakening of the reef framework and subsequent degradation of the complex coral reef ecosystem.

Data availability

The datasets generated during and/or analysed during the current study are available from the corresponding author on reasonable request.

Received: 30 December 2020; Accepted: 6 September 2021

Published online: 07 October 2021

References

- Hoegh-Guldberg, O. *et al.* Coral reefs under rapid climate change and ocean acidification. *Science* (80-) **318**, 1737–1742 (2007).
- Roberts, M., Hanley, N., Williams, S. & Cresswell, W. Terrestrial degradation impacts on coral reef health: Evidence from the Caribbean. *Ocean Coast. Manag.* **149**, 52–68 (2017).
- Mollica, N. R. *et al.* Ocean acidification affects coral growth by reducing skeletal density. *Proc. Natl. Acad. Sci.* **115**, 1754–1759 (2018).
- Ries, J. B. Skeletal mineralogy in a high-CO₂ world. *J. Exp. Mar. Biol. Ecol.* **403**, 54–64 (2011).
- Erez, J., Reynaud, S., Silverman, J., Schneider, K. & Allemand, D. Coral calcification under ocean acidification and global change. In *Coral Reefs: An Ecosystem in Transition* (2011). https://doi.org/10.1007/978-94-007-0114-4_10.
- Dove, S. G. *et al.* Future reef decalcification under a business-as-usual CO₂ emission scenario. *Proc. Natl. Acad. Sci.* **110**, 15342–15347 (2013).
- Cooper, T. F., De'ath, G., Fabricius, K. E. & Lough, J. M. Declining coral calcification in massive *Porites* in two nearshore regions of the northern Great Barrier Reef. *Glob. Chang. Biol.* **14**, 529–538 (2008).
- Cooper, T. F., O'Leary, R. A. & Lough, J. M. Growth of Western Australian corals in the Anthropocene. *Science* (80-) **335**, 593–596 (2012).
- Teixidó, N. *et al.* Ocean acidification causes variable trait-shifts in a coral species. *Glob. Chang. Biol.* <https://doi.org/10.1111/gcb.15372> (2020).
- Pandolfi, J. M. Incorporating uncertainty in predicting the future response of coral reefs to climate change. *Annu. Rev. Ecol. Evol. Syst.* **46**, 281–303 (2015).
- Kroeker, K. J., Kordas, R. L., Crim, R. N. & Singh, G. G. Meta-analysis reveals negative yet variable effects of ocean acidification on marine organisms. *Ecol. Lett.* **13**, 1419–1434 (2010).
- Jokiel, P. L. *et al.* Ocean acidification and calcifying reef organisms: A mesocosm investigation. *Coral Reefs* **27**, 473–483 (2008).
- Fantazzini, P. *et al.* Gains and losses of coral skeletal porosity changes with ocean acidification acclimation. *Nat. Commun.* **6**, 7785 (2015).
- Wittmann, A. C. & Pörtner, H.-O. Sensitivities of extant animal taxa to ocean acidification. *Nat. Clim. Chang.* **3**, 995–1001 (2013).
- Fabricius, K. E. *et al.* Losers and winners in coral reefs acclimatized to elevated carbon dioxide concentrations. *Nat. Clim. Chang.* **1**, 165–169 (2011).
- Riebesell, U. Acid test for marine biodiversity. *Nature* **454**, 46–47 (2008).
- Hall-Spencer, J. M. *et al.* Volcanic carbon dioxide vents show ecosystem effects of ocean acidification. *Nature* **454**, 96–99 (2008).
- Johnson, V. R., Russell, B. D., Fabricius, K. E., Brownlee, C. & Hall-Spencer, J. M. Temperate and tropical brown macroalgae thrive, despite decalcification, along natural CO₂ gradients. *Glob. Chang. Biol.* <https://doi.org/10.1111/j.1365-2486.2012.02716.x> (2012).
- Prada, F. *et al.* Ocean warming and acidification synergistically increase coral mortality. *Sci. Rep.* **7**, 1–10 (2017).
- Inoue, S., Kayanne, H., Yamamoto, S. & Kurihara, H. Spatial community shift from hard to soft corals in acidified water. *Nat. Clim. Chang.* **3**, 683–687 (2013).

21. Crook, E. D., Cohen, A. L., Rebolledo-Vieyra, M., Hernandez, L. & Paytan, A. Reduced calcification and lack of acclimatization by coral colonies growing in areas of persistent natural acidification. *Proc. Natl. Acad. Sci.* **110**, 11044–11049 (2013).
22. Teixidó, N. *et al.* Functional biodiversity loss along natural CO₂ gradients. *Nat. Commun.* **9**, 5149 (2018).
23. Strahl, J. *et al.* Physiological and ecological performance differs in four coral taxa at a volcanic carbon dioxide seep. *Comp. Biochem. Physiol. Part A Mol. Integr. Physiol.* **184**, 179–186 (2015).
24. Fabricius, K. E., De'ath, G., Noonan, S. & Uthicke, S. Ecological effects of ocean acidification and habitat complexity on reef-associated macroinvertebrate communities. *Proc. R. Soc. B Biol. Sci.* **281**, 20132479 (2014).
25. Fabricius, K. E., Noonan, S. H. C., Abrego, D., Harrington, L. & De'ath, G. Low recruitment due to altered settlement substrata as primary constraint for coral communities under ocean acidification. *Proc. R. Soc. B Biol. Sci.* **284**, 20171536 (2017).
26. Siahainenia, L., Tuhumury, S. F., Uneputti, P. A. & Tuhumury, N. C. Survival and growth of transplanted coral reef in lagoon ecosystem of Ihamahu, Central Maluku, Indonesia. *IOP Conf. Ser. Earth Environ. Sci.* **339**, 012003 (2019).
27. Horwitz, R., Hoogenboom, M. O. & Fine, M. Spatial competition dynamics between reef corals under ocean acidification. *Sci. Rep.* **7**, 40288 (2017).
28. Noonan, S. H. C., Fabricius, K. E. & Humphrey, C. *Symbiodinium* community composition in scleractinian corals is not affected by life-long exposure to elevated carbon dioxide. *PLoS ONE* **8**, e63985 (2013).
29. Caroselli, E. *et al.* Environmental implications of skeletal micro-density and porosity variation in two scleractinian corals. *Zoology* **114**, 255–264 (2011).
30. Reggi, M. *et al.* Biomineralization in Mediterranean corals: The role of the intraskeletal organic matrix. *Cryst. Growth Des.* **14**, 4310–4320 (2014).
31. Goffredo, S. *et al.* The skeletal organic matrix from Mediterranean coral *Balanophyllia europaea* influences calcium carbonate precipitation. *PLoS ONE* **6**, e22338 (2011).
32. Goffredo, S. *et al.* Biomineralization control related to population density under ocean acidification. *Nat. Clim. Chang.* **4**, 593–597 (2014).
33. Borgia, G. C., Brown, R. J. S. & Fantazzini, P. Uniform-penalty inversion of multiexponential decay data. *J. Magn. Reson.* **132**, 65–77 (1998).
34. Bortolotti, F., Brown, R. & Fantazzini, P. *OpenWin: A Software for Inversion of Multiexponential Decay Data* (Windows System Alma Mater Studiorum—Università di Bologna, 2012).
35. Fantazzini, P. *et al.* A time-domain nuclear magnetic resonance study of Mediterranean scleractinian corals reveals skeletal-porosity sensitivity to environmental changes. *Environ. Sci. Technol.* **47**, 12679–12686 (2013).
36. Coronado, I., Fine, M., Bosellini, F. R. & Stolarski, J. Impact of ocean acidification on crystallographic vital effect of the coral skeleton. *Nat. Commun.* **10**, 2896 (2019).
37. Pokroy, B., Fitch, A. & Zolotoyabko, E. The microstructure of biogenic calcite: A view by high-resolution synchrotron powder diffraction. *Adv. Mater.* **18**, 2363–2368 (2006).
38. Anderson, M. J., Gorley, R. N. & Clarke, K. R. PERMANOVA+ for PRIMER: Guide to software and statistical methods. In *Plymouth* (2008).
39. R Development Core Team. *R: A Language and Environment for Statistical Computing* (R Foundation for Statistical Computing, 2018). ISBN 3-900051-07-0. <http://www.R-project.org>.
40. Toby, B. H. & Von Dreele, R. B. GSAS-II: The genesis of a modern open-source all purpose crystallography software package. *J. Appl. Crystallogr.* **46**, 544–549 (2013).
41. Jiang, H. G., Rühle, M. & Laverna, E. J. On the applicability of the x-ray diffraction line profile analysis in extracting grain size and microstrain in nanocrystalline materials. *J. Mater. Res.* **14**, 549–559 (1999).
42. Vercelloni, J. *et al.* Forecasting intensifying disturbance effects on coral reefs. *Glob. Chang. Biol.* **26**, 2785–2797 (2020).
43. Guo, W. *et al.* Ocean acidification has impacted coral growth on the Great Barrier Reef. *Geophys. Res. Lett.* **47**, 1–9 (2020).
44. Tambutté, E. *et al.* Morphological plasticity of the coral skeleton under CO₂-driven seawater acidification. *Nat. Commun.* **6**, 7368 (2015).
45. Schneider, K. & Erez, J. The effect of carbonate chemistry on calcification and photosynthesis in the hermatypic coral *Acropora eurystoma*. *Limnol. Oceanogr.* **51**, 1284–1293 (2006).
46. Martinez, A. *et al.* Species-specific calcification response of Caribbean corals after 2-year transplantation to a low aragonite saturation submarine spring. *Proc. Biol. Sci.* **286**, 20190572 (2019).
47. Comeau, S. *et al.* Resistance to ocean acidification in coral reef taxa is not gained by acclimatization. *Nat. Clim. Chang.* **9**, 477–483 (2019).
48. McCulloch, M. *et al.* Resilience of cold-water scleractinian corals to ocean acidification: Boron isotopic systematics of pH and saturation state up-regulation. *Geochim. Cosmochim. Acta* **87**, 21–34 (2012).
49. Movilla, J. *et al.* Differential response of two Mediterranean cold-water coral species to ocean acidification. *Coral Reefs* **33**, 675–686 (2014).
50. Kurihara, H., Takahashi, A., Reyes-Bermudez, A. & Hidaka, M. Intraspecific variation in the response of the scleractinian coral *Acropora digitifera* to ocean acidification. *Mar. Biol.* **165**, 38 (2018).
51. Barnes, D. J. & Devereux, M. J. Variations in skeletal architecture associated with density banding in the hard coral *Porites*. *J. Exp. Mar. Biol. Ecol.* **121**, 37–54 (1988).
52. Bucher, D. J., Harriott, V. J. & Roberts, L. G. Skeletal micro-density, porosity and bulk density of acroporid corals. *J. Exp. Mar. Biol. Ecol.* **228**, 117–136 (1998).
53. Mass, T. *et al.* Amorphous calcium carbonate particles form coral skeletons. *Proc. Natl. Acad. Sci.* **114**, E7670–E7678 (2017).
54. Vidal-Dupiol, J. *et al.* Genes related to ion-transport and energy production are upregulated in response to CO₂-driven pH decrease in corals: New insights from transcriptome analysis. *PLoS ONE* **8**, e58652 (2013).
55. Suggett, D. J. *et al.* Light availability determines susceptibility of reef building corals to ocean acidification. *Coral Reefs* **32**, 327–337 (2013).
56. Vogel, N., Meyer, F., Wild, C. & Uthicke, S. Decreased light availability can amplify negative impacts of ocean acidification on calcifying coral reef organisms. *Mar. Ecol. Prog. Ser.* **521**, 49–61 (2015).
57. Tanaka, Y. *et al.* Nutrient availability affects the response of juvenile corals and the endosymbionts to ocean acidification. *Limnol. Oceanogr.* **59**, 1468–1476 (2014).
58. Towle, E. K., Enochs, I. C. & Langdon, C. Threatened Caribbean coral is able to mitigate the adverse effects of ocean acidification on calcification by increasing feeding rate. *PLoS ONE* **10**, e0123394 (2015).
59. Stolarski, J., Przeniosło, R., Mazur, M. & Brunelli, M. High-resolution synchrotron radiation studies on natural and thermally annealed scleractinian coral biominerals. *J. Appl. Crystallogr.* **40**, 2–9 (2007).
60. Maslen, E. N., Streltsov, V. A., Streltsova, N. R. & Ishizawa, N. Electron density and optical anisotropy in rhombohedral carbonates. III. Synchrotron X-ray studies of CaCO₃, MgCO₃ and MnCO₃. *Acta Crystallogr. Sect. B Struct. Sci.* **51**, 929–939 (1995).
61. Wall, M. *et al.* Linking internal carbonate chemistry regulation and calcification in corals growing at a Mediterranean CO₂ vent. *Front. Mar. Sci.* **6**, 699 (2019).
62. Wickham, H. *ggplot2* (Springer International Publishing, 2016). <https://doi.org/10.1007/978-3-319-24277-4>.

Acknowledgements

We would like to thank the communities at Upa Upasina and at Dobu to allow us to work at their unique reefs. Many thanks also to Craig Humphrey and Sam Noonan for collecting the samples. The field research was funded by the Australian Institute of Marine Science.

Author contributions

K.E.F. designed the experimental setting, initiated the collection of the specimens, and provided the background environmental data. F.P., L.B., S.Fe., I.P., N.B., F.R., Q.P., B.P., and L.G. analyzed the samples. FP, SFr, and EC performed the statistical analyses. F.P., L.B., S.Fr., S.M., and P.F. contributed to the initial draft. F.P., L.B., S.Fr., S.M., N.B., E.C., Z.D., P.F., G.F., S.G., and K.E.F. contributed to the scientific discussion and interpretation of the data. All authors contributed to writing the manuscript and gave final approval for publication.

Competing interests

The authors declare no competing interests.

Additional information

Supplementary Information The online version contains supplementary material available at <https://doi.org/10.1038/s41598-021-98976-9>.

Correspondence and requests for materials should be addressed to P.F., G.F. or S.G.

Reprints and permissions information is available at www.nature.com/reprints.

Publisher's note Springer Nature remains neutral with regard to jurisdictional claims in published maps and institutional affiliations.



Open Access This article is licensed under a Creative Commons Attribution 4.0 International License, which permits use, sharing, adaptation, distribution and reproduction in any medium or format, as long as you give appropriate credit to the original author(s) and the source, provide a link to the Creative Commons licence, and indicate if changes were made. The images or other third party material in this article are included in the article's Creative Commons licence, unless indicated otherwise in a credit line to the material. If material is not included in the article's Creative Commons licence and your intended use is not permitted by statutory regulation or exceeds the permitted use, you will need to obtain permission directly from the copyright holder. To view a copy of this licence, visit <http://creativecommons.org/licenses/by/4.0/>.

© The Author(s) 2021